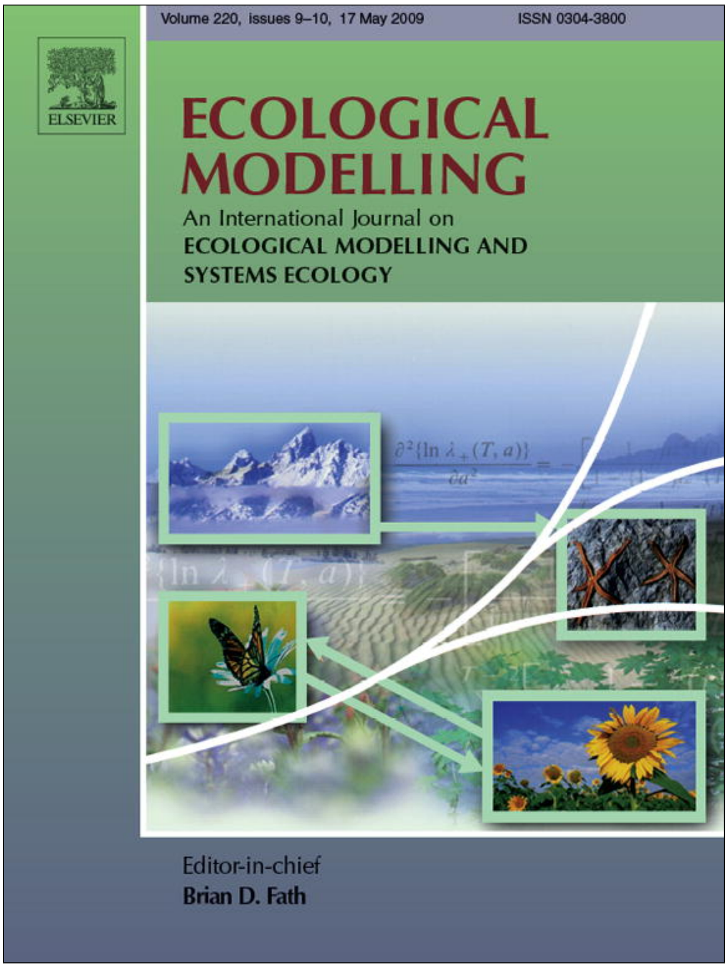
Volume 220, issues 9–10, 17 May 2009
ISSN 0304-3800
ELSEVIER
ECOLOGICAL MODELLING
An International Journal on
ECOLOGICAL MODELLING AND SYSTEMS ECOLOGY
Editor-in-chief
Brian D. Fath

Ecological Modelling 220 (2009) 1325–1338

Contents lists available at ScienceDirect

Ecological Modelling

journal homepage: www.elsevier.com/locate/ecolmodel

Modelling carbon storage in highly fragmented and human-dominated landscapes: Linking land-cover patterns and ecosystem models

D.T. Robinson*, D.G. Brown, W.S. Currie

School of Natural Resources and Environment, University of Michigan, 440 Church Street, Ann Arbor, MI 48109-1041, United States

ARTICLE INFO

Article history:
Received 15 September 2008
Received in revised form 17 February 2009
Accepted 18 February 2009
Available online 25 March 2009

Keywords:
BIOME-BGC
Carbon cycling
Fragmentation
Eastern deciduous forests
Edge effects
Ecosystem process modelling
Within-patch heterogeneity
Land-use and land-cover change

ABSTRACT

To extend coupled human–environment systems research and include the ecological effects of land-use and land-cover change and policy scenarios, we present an analysis of the effects of forest patch size and shape and landscape pattern on carbon storage estimated by BIOME-BGC. We evaluate the effects of including within-patch and landscape-scale heterogeneity in air temperature on carbon estimates using two modelling experiments. In the first, we combine fieldwork, spatial analysis, and BIOME-BGC at a 15-m resolution to estimate carbon storage in the highly fragmented and human-dominated landscape of Southeastern Michigan, USA. In the second, we perform the same analysis on 12 hypothetical landscapes that differ only in their degree of fragmentation. For each experiment we conduct four air-temperature treatments, three guided by field-based data and one empirically informed by local National Weather Service station data. The three field data sets were measured (1) exterior to a forest patch, (2) from the patch edge inward to 60 m on east-, south-, and west-facing aspects, separately, and (3) interior to that forest patch. Our field-data analysis revealed a decrease in maximum air temperature from the forest patch edge to a depth of 80 m. Within-patch air-temperature values were significantly different ($\alpha = 0.01$) among transects (c.v. = 13.28) and for all measurement locations (c.v. = 30.58). Results from the first experiment showed that the interior treatment underestimated carbon storage by ~8000 Mg C and the exterior treatment overestimated carbon storage by 30,000 Mg C within Dundee Township, Southeastern Michigan, when compared to a treatment that included within-patch heterogeneity. In the second experiment we found a logarithmic increase in carbon storage with increasing fragmentation ($r^2 = 0.91$). While a number of other processes (e.g. altered disturbance frequency or severity) remain to be included in future experiments, this combined field and modelling study clearly demonstrated that the inclusion of within-patch and landscape heterogeneity, and landscape fragmentation, each have a strong effect on forest carbon cycling and storage as simulated by a widely used ecosystem process model.

1. Introduction

Processes of land-use and land-cover change (LUCC) are characterized by local complexities and feedbacks that produce global consequences (Foley et al., 2005), including effects on climate (Houghton et al., 1999; Schimel et al., 2000; Barford et al., 2001). The alteration of the earth's surface changes the albedo (Pielke et al., 2002); sensible and latent heat flux; evaporation (Betts et al., 1996); biodiversity (Poschlod et al., 2005); biophysical characteristics that contribute to nutrient and hydrological cycling (Hubacek and Vazquez, 2002); and carbon (C) storage (Dixon et al., 1994). Each of these biophysical functions significantly influence global climate (Riebsame et al., 1994). Globally, land-use change in the 1980s and 1990s contributed 1.4[1] and 1.6 Pg C yr^{-1} to the atmosphere (1 Pg = 10^{15} g = 1 Gt) and represented approximately 30% of anthropogenic efflux of carbon to the atmosphere (Dixon et al., 1994). Conversely, mid-to-high latitude forest expansion driven by reduced agricultural land use in the 1990s (Gower, 2003) contributed to a net carbon sink by land-use within these regions (Fan et al., 1998; Caspersen et al., 2000).

Because LUCC is complex and driven by human activities, understanding its' effects on ecosystem processes involves studying a coupled human–environment system. To date, a number of projects have determined the dominant mechanisms influencing these coupled systems and in some cases mapped (with measured error)

* Corresponding author. Tel.: +1 734 276 1130; fax: +1 734 936 2195.
E-mail address: dtrobins@umich.edu (D.T. Robinson).

[1] Land-use change flux based on Chapter 7 of the 2007 Intergovernmental Panel on Climate Change (IPCC) report, which noted the land-use change induced carbon efflux to the atmosphere to be 1.4 (0.4–2.3) Pg C yr^{-1} for the 1980s and 1.6 (0.5–2.7) Pg C yr^{-1} for the 1990s. Values in parentheses represent range of uncertainty.

0304-3800/$ – see front matter © 2009 Elsevier B.V. All rights reserved.
doi:10.1016/j.ecolmodel.2009.02.020

observed spatial patterns of LUCC (e.g. Deadman et al., 2004; Huigen, 2004). However, most LUCC projects fall short by failing to incorporate measurements of key ecological functions (e.g. biogeochemical cycling) and how those functions affect and are affected by human systems. It is necessary to represent both of these types of interactions if we wish to assess the influence of local LUCC on global climate change. This problem is recognized by a number of government agencies and affiliations (e.g. Turner et al., 1995; Lambin et al., 1999; Gimblett, 2002; Parker et al., 2002; Lobo, 2004; Gutman et al., 2004; GLP, 2005).

Paralleling LUCC initiatives are ecological studies that use models to explore the effects of succession, disturbance, competition, biophysical changes, and geography on ecosystem structure, function, and biodiversity (Parton et al., 1987; Jeltsch et al., 1996; He et al., 1999a,b; Gustafson et al., 2000; Shugart, 2000; Urban and Keitt, 2001; Howe and Baker, 2003). Ecosystem process models that focus on biogeochemical cycling have found utility in global climate change research because they are typically applied at resolutions $\geq$1 km^2 and can quantify evapotranspiration, water use efficiency, carbon (C) and other nutrient pools and fluxes. In contrast to the coarse-scale resolution ($\geq$1 km^2) typically employed by ecosystem process models, some models such as BIOME-BGC or 3-PG have been successfully applied at a resolution of 30 m (Coops and Waring, 2001). While successfully applied at relatively fine resolutions, few if any such models incorporate the effects of ecosystem patch edge, shape (e.g. irregular forest patch perimeters), size, or edge-to-area ratios on ecosystem function. Therefore, applying a model such as BIOME-BGC to simulate forest C in two landscapes with equal forest area, but different spatial pattern, would produce equal amounts of total forest carbon.

However, microclimate and biophysical characteristics are altered along a transition zone between the adjacent ecosystem (e.g. prairie) and the forest interior (Matlack, 1993) on the scale of tens to hundreds of meters. On exposed forest patch edges, light and wind may penetrate beneath closed canopies causing gradient changes in temperature, moisture, and the vapour pressure deficit deep into the forest (Chen et al., 1995). The depth of penetration and alteration of climate characteristics is a function of forest type, structural characteristics (e.g. stem density), aspect, and side-canopy presence (Matlack, 1993). For eastern deciduous forests these effects have been observed to penetrate into patches in the range 15–50 m, while edge-effect penetration has been observed to be greater than 240 m in Douglas fir forests (Chen et al., 1995).

In addition to edge effects, landscape heterogeneities in the form of patch shape, patch size, landform, and proximal land use and land cover may influence local climate. For example, the perimeter/area ratio of a patch along with patch size can describe the degree of core area of a forest patch that is buffered by local climate (Collinge, 1996). The physical characteristics of the landscape (i.e. landform) such as slope and aspect influence the degree of incident solar radiation; elevation influences adiabatic processes; and proximity to water features can influence humidity levels, each of which can affect local climate (Rosenberg et al., 1983). Similarly, different types of land uses and land covers have also been shown to influence local climate (Landsberg, 1970). For example, urban heat islands have extended influence on temperature values beyond city limits (Arnfield, 2003) and agricultural lands can affect heat fluxes and influence thunderstorm frequency (Raddatz, 2007).

As a step towards integrating LUCC and ecosystem models focused on biogeochemical cycling, we addressed issues of edge and landscape heterogeneity, whereby the landscape is composed of forest patches of variable shapes and sizes within a matrix of other types of land cover. Our research addresses two specific questions through analysis of ecological field data, its subsequent incorporation into BIOME-BGC, and application to the heterogeneous landscape of Southeastern Michigan. The primary question is: How does a more realistic treatment of forest patch size and shape in a fragmented and human-dominated landscape, through microclimate edge effects, alter calculations of the forest carbon balance using the ecosystem process model BIOME-BGC? In order to address this question we additionally explore: What are the spatial and temporal differences in air temperature in forest patch edges and interior in a particular human-dominated landscape, and how far into a typical forest patch do these microclimatic differences penetrate?

2. Materials and methods

2.1. Study area

Our study area was located within the heterogeneous, fragmented, and human-dominated landscape of Southeastern Michigan. Forest patches in this region primarily exist as secondary growth forest, remnants of abandoned agricultural land. Agriculture peaked as a land use in the area in the late 1880s to 1900 and has declined from 1910 to the present. Since then, heterogeneity of the landscape has been increasing due to LUCC at the urban–rural interface. While the region is representative of land-use histories and land-cover patterns of the Midwest and populated regions in the eastern temperate zone of North America, we chose a single township (i.e. Dundee Township, in Monroe County, Southeastern Michigan, USA) 12,577 ha in area, as our study area to conduct both field work and model application (Fig. 1).

In 2001, approximately 10% (1277.28 ha) of the study area was forested (Homer et al., 2007—NLCD data). The amount of forest in Dundee Township was below average for Southeastern Michigan where the mean during the same time period was 28% forest (standard deviation 13%) based on 140 townships sampled from the 10 adjoining counties (Genesee, Lapeer, Lenawee, Livingston, Macomb, Monroe, Oakland, St. Clair, Washtenaw, and Wayne). Dundee Township illustrates the extent to which the regional landscape has been modified, fragmented, and become dominated by anthropogenic land uses. The township is now composed of 262 forest patches in an agricultural and residential matrix with a mean forest patch size of 5.02 ha (standard deviation 10.45 ha). The total patch edge in Dundee Township is 398 km and the edge density (total edge/total landscape area) is 31.64 m ha^{-1}.

From within Dundee Township we chose a single forest patch, typical of the region, to conduct our field study. The forest patch provided ideal characteristics to study changes in daily minimum and maximum temperatures from the forest patch edge inward. Our field study patch consisted of a single, privately owned, eastern deciduous forest patch that was situated (1) 0.5 km from the nearest creek and 0.7 km from other tree cover, (2) on a slope less than 3°, and (3) within a uniform surrounding vegetation (i.e. corn and soy crops). The edges of the selected patch were linear, partially closed side-canopy, and perpendicular to the cardinal directions. The 220 m $\times$ 210 m (4.62 ha) forest patch was approximately 80 years in age with a canopy height of 24–30 m. The dimensions of the patch ensured that measurement points were not located where the influence of two adjacent edges could overlap. To the best of our knowledge the patch had not experienced any significant major disturbance in the past 80 years, although some wind throw is a normal part of the disturbance regime in this region (Frelich, 2002) and did occur along two of our three transects during our study period.

Our field study patch was located within the Maumee Lake Plain ecosystem type (Albert, 1995), which runs across much of the eastern boarder of Southeast Michigan. Forests in this ecosystem are characterized by beech-sugar maple or elm-ash species (Albert, 1995). The loamy sand on which the site is located was produced from glacial outwash sand and gravel, postglacial alluvium, and

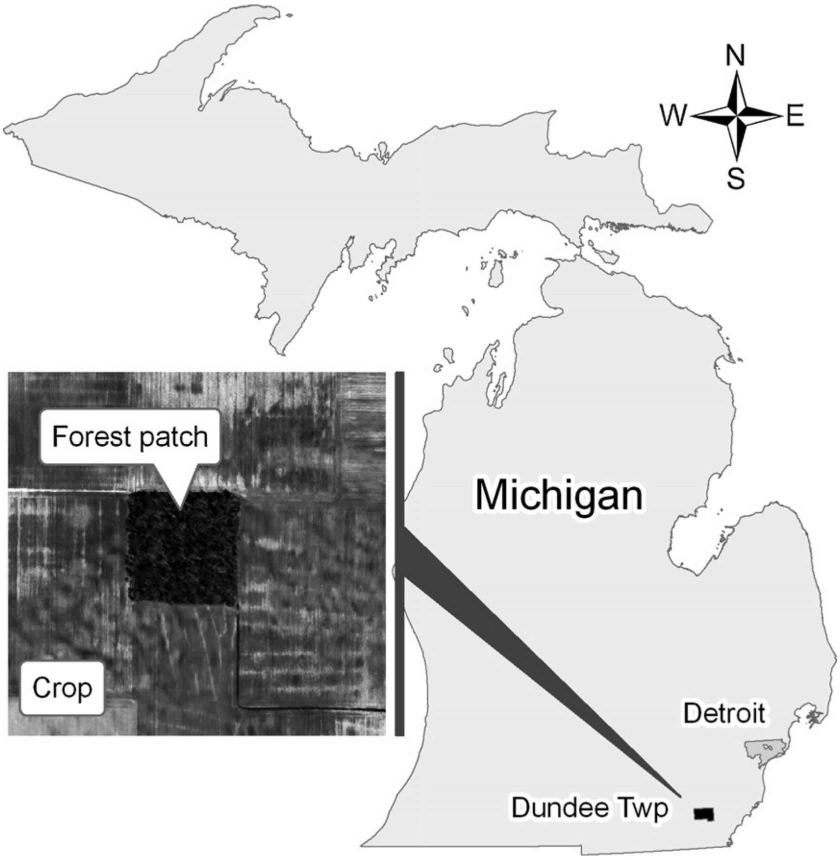

Fig. 1. Aerial photo of study forest patch taken in year 2000 and location of study area Dundee Township, Michigan, USA.

coarse-textured till from end moraines. These soil and surficial geologic conditions are typical of Southeastern Michigan.

2.2. Field data collection and analysis

The objective of our field-data collection and analysis was to statistically determine if there was a difference in minimum and maximum air temperature among locations from the edge of an eastern deciduous forest patch inward to forest interior. We performed two analyses to test whether air temperature differed with forest depth. To accommodate our repeated measures of more than two dependent samples, we first performed a non-parametric Friedman two-way analysis of variance by ranks test (Sheskin, 2004). Using observed air temperature as the response variable, sensor locations as the treatments, and observations blocked by day and hour, we calculated a chi-square (χ^2) value for maximum and minimum air-temperature observations for each transect and all sensors combined. Second, we performed a functional data analysis to further illustrate the direction of the temperature gradient from the forest patch edge inward to the forest interior. A functional data analysis was conducted by creating a simple linear model of temperature as a function of distance for each point in time, which took the following form:

$$T_{obs} = a + m(d - d_{ave}) \quad (1)$$

where T_{obs} is the observed temperature, a the intercept, m the slope, d the distance the temperature measurement was taken from the forest edge into the interior, and d_{ave} is the average of the distance measurements. We performed a linear regression of the six temperature values (i.e. taken at 0, 15, 30, 45, 60 m, and at the forest interior 80 m) to model the change in slope and intercept with respect to distance for each hourly measurement.

Field-data collection focused on maximum and minimum air-temperature observations because these two climate parameters can be used by the MTCLIM model (Running et al., 1987; Thornton and Running, 1999), which accompanies BIOME-BGC, to produce the climate variables needed to execute BIOME-BGC (i.e. minimum and maximum temperature, daylight average temperature, short-wave solar radiation, vapour pressure deficit, and day length). Three transects corresponding to east, south, and west aspects were established at the forest patch edge extending to a depth of 60 m within the forest patch. Due to a number of limitations we did not evaluate the edge effects from the northern edge; however other studies have suggested that there is little to no effect on the northern edge in the northern hemisphere (Matlack, 1993). Transects were located beyond 60 m from a patch corner to prevent edge overlap. Existing literature suggests that abiotic edge gradients often cease to extend beyond 50–60 m in eastern deciduous forests (Matlack, 1993; Cadenasso et al., 1997). At each measurement point, temperature was recorded at 15.25 m (50 ft) aboveground and approximately 1 m from the stem on the south side of a live tree. Temperature measurements were recorded every 15 min at the forest edge and distances approximating 0, 15, 30, 45, and 60 m inside the forest along each transect. The data reported in this paper include hourly maximum and minimum air temperature for all hours from 15 May to 31 August 2006, using Hobo Pro Temp/RH data loggers produced by Onset (www.onsetcomp.com).

An additional measurement point was located within the forest at a depth of approximately 80 m from the south-facing edge (to provide a measure of patch interior temperature) and a second additional measurement point was placed external to the forest patch to replicate standard meteorological measures of air temperature. The external measurement point was located between two agricultural fields (soybean and corn) along a section of turf

Table 1
Above ground biomass and carbon (C) content measurements for eastern deciduous broadleaf forests.

Source	Location	Dominant overstory species	Forest tpe	Biomass ($kg\,m^{-2}$)	Carbon ($kg\,m^{-2}$)	NPP ($Mg\,C\,ha^{-1}\,yr^{-1}$)	LAI ($m^2\,m^{-2}$)
Botkin et al. (1993)[a]	Eastern North America	Across 13 physiographic regions	Temperate Deciduous	8.1 ± 1.4	3.6 ± 0.6	–	–
Botkin et al. (1993)[b]	Eastern North America	Across 13 physiographic regions	Temperate Deciduous	9.8 ± 1.8	4.4 ± 0.8	–	–
Botkin et al. (1993)[c]	Eastern North America	Across 13 physiographic regions	Temperate Deciduous	9.2 ± 1.6	4.1 ± 0.7	–	–
Bolstad et al. (2001)	Coweeta Hydrologic Laboratory, Western North Carolina, USA	Chestnut oak (*Quercus prinus*), red maple (*Acer rubrum* L.), (*Catya*), and American tulip tree (*Liriodendron tulipifera*)	Eastern North American Deciduous	–	–	9.20	2.7–8.2
Curtis et al. (2002)	Walker Branch, Eastern Tennessee, USA	White oak (*Quercus alba* L.), red maple, sugar maple (*Acer saccharum* Marchall.), and American tulip tree	Eastern North American Deciduous	21.63[d]	9.73	5.39	6.2
Curtis et al. (2002)	Morgan Monroe State Forest, South-central Indiana, USA	Sugar maple, yellow poplar, sassafras (*Sassafras atbidum* Nutt.), white oak, and black oak (*Quercus velutina* Lam.)	Eastern North American Deciduous	22.65[d]	10.19	5.29	4.9
Curtis et al. (2002)	Harvard Forest, North-central Massachusetts, USA	Red oak (*Quercus rubra* L.), black oak, red maple, hemlock (*Tsuga canadensis* L.), white pine (*Pinus strobus* L.) and red pine (*Pinus resinosa* Aiton.) plantations	Eastern North American Deciduous	23.34[d]	10.50	3.20	4.0
Curtis et al. (2002)	University of Michigan Biological Station, Northern Lower Michigan	Bigtooth aspen (*Populus grandidentata* Michx.), Trembling aspen (*Populus tremuloides* Michx.), red oak, beech (*Fagus grandifotia* Ehrh.), sugar maple, white pine, and hemlock	Eastern North American Deciduous	13.83[d]	6.22[e]	3.38	3.7
Curtis et al. (2002)	Willow creek, North-central Wisconsin, USA	Sugar maple, American basswood (*Tilia americana* L.), green ash (*Fraxinus pennsyivanica* Marsh.), and red oak	Eastern North American Deciduous	17.47[d]	7.86	3.00	4.2
Newman et al. (2006)	Southeastern Kentucky, USA	Cucumber magnolia (*Magnolia acuminata*), American tulip tree, sugar maple, American basswood, red oak, red maple	Mesic Deciduous	24.08[d]	10.83	5.13–11.56[f]	7.9
Newman et al. (2006)	Southeastern Kentucky, USA	Chesnut oak (*Q. prinus*), Scarlet oak (*Quercus coccinea*), black oak (*Quercus veluntina*), red maple, red oak, white oak	Xeric Deciduous	24.68[d]	11.10	5.13–11.56[f]	3.5
Average				17.48	7.85		4.3
This study[g]	Southeastern Lower Michigan, USA	American basswood, American elm (*Ulmus americana*), red maple, Swamp white oak (*Quercus bcolor*), hawthorn (*Crataegus monogyna*), red oak, Bitternut hickory (*Carya cordiformis*), white ash (*Fraxinus americana*), and silver maple (*Acer saccbarinum*)	Eastern North American Deciduous	19.12	8.61	–	3.36
This study[h]	Southeastern Lower Michigan, USA		Eastern North American Deciduous	21.44	9.65	–	3.26

(–) No available data reported.
[a] Values of Botkin et al. (1993) are lower than others due their random sampling which included young forest.
[b] Use of general hardwoods biomass equations from Clark et al. (1986a) on all angiosperms.
[c] Use of general hardwoods biomass equations from Clark et al. (1986b) on all angiosperms.
[d] Calculated from reported C values.
[e] Foliage and understory omitted.
[f] Range over several sites.
[g] Average of subplots.
[h] Total forest patch average.

grass used for transportation by the property owner. The external sensor was located approximately 4.5 m above the ground on a wooden pole erected away from shade and above the average fully grown corn stalk of approximately 2.5 m. Each sensor was covered by a rain shield to prevent direct contact by sunlight and moisture.

In addition to air-temperature measurements, a number of independent site variables were recorded along each transect and surrounding each forest canopy measurement point. These variables included distance from edge, basal area of trees with a diameter at breast height (dbh) >1.5 cm (conducted on 17 September 2006), and leaf area index (LAI). A number of 10 m × 10 m plots were established, centered on each forest canopy measurement point, in a line inward from the patch edge. Plots located on the patch edge had a dimension of 10 m × 5 m. LAI measurements were taken on 18 August 2006, using an LAI 2000 plant canopy analyzer produced by LI-COR Biosciences. Three readings external to the forest, using a 180° lens cap to block residual backscatter from the forest, were taken first. Then eight readings were taken within each plot from which an average LAI value was calculated (LI-COR, 1992). This process was repeated for each plot.

Individual tree biomass was estimated using allometric equations of the form $M = aD^b$ where M is the oven-dry weight (kg) of biomass, D is the dbh (cm), and a and b are parameters based on previous empirical research (Ter-Mikaelian and Korzukhin, 1997). We used two methods to extrapolate biomass values up to the patch level and then divided the result by the patch area to obtain biomass in kg m^{-2} (Table 1). Content of carbon was calculated as 45% of the oven-dry biomass (Whittaker, 1975) to coincide with previously published values; however, others have shown percent carbon can be higher (e.g. Currie et al., 2003; Gower, 2003). GPP values for Southeastern Michigan were obtained at a coarse resolution of 1 km^2 using remote sensing techniques (Zhao et al., 2007). The authors used the light use efficiency (LUE or ε) from BIOME-BGC to estimate GPP and derived a value of 759 g C m^{-2} in 1999 (Zhao et al., 2007).

2.3. Calibration and parameterization of BIOME-BGC

Our desire to integrate land-cover data and forest ecosystem processes at a fine resolution (15 m) was met by using BIOME-BGC. The model was developed to determine if a single ecosystem process model could be useful for representing biogeochemical cycling in multiple biome types (Running and Hunt, 1993). BIOME-BGC simulates multiple C storage and flux outputs and partitions storage and respiration into individual pools (e.g. canopy, stem, and roots) as well as ecosystem level outputs such as gross photosynthesis and net primary production (NPP) (Running and Coughlan, 1988; Running and Hunt, 1993).

The process of using BIOME-BGC required us to first perform a spin-up simulation, which slowly grew a simulated forest on the landscape until a dynamic equilibrium was met among climate, vegetation ecophysiology, soil organic matter (SOM), and nutrient pools (Thornton et al., 2002). The spin-up phase produced a restart file that described the state of the ecosystem and facilitated future runs of the model without re-establishing system equilibrium each run. Because land-use history (e.g. agriculture) affects the size of C and N pools above and below ground in present-day forest patches in the region, we altered the restart file to represent the agricultural land-use history of Dundee Township. We re-initialized C and N content in litter, live and dead forest stems, and coarse woody debris to 1% of their equilibrium value. We then initialized soil C and N in the fast microbial recycling pool to 1% and decreased the medium and slow microbial C and N pools by 30% and 15%, respectively, to reflect the alteration to soil as reported in the literature (Table 2). Then we were able to simulate forest stand growth from 1930 to 2006, which approximated the age of our forest site growing on prior agricultural land.

Typical calibration procedures involve comparing model output such as LAI and GPP to site-specific observations (e.g. Jung et al., 2007). We used chi-square statistics (χ^2) and altered two ecophysiological parameters to calibrate BIOME-BGC by assessing the goodness of fit between our study site observations of LAI (3.36 m m^{-2}), above-ground carbon storage (9.13 kg C m^{-2}, average of values estimated in Table 1), and 1999 GPP (759 g C m^{-2}) with our model output. We also wanted to restrain the number of parameter alterations of the default deciduous broadleaf biome, which has been established as generally representative of the eastern deciduous biome and undergone significant testing (White et al., 2000). Similar to Tatarinov and Cienciala (2006), we increased the rate of annual whole-plant mortality from 0.005 to 0.01, which is a 1% per year mortality rate. We increased the mortality rate to represent the increased mortality due to wind-throw, insect infestation, and disease that occur more frequently in fragmented and human-dominated landscapes. We also increased the fraction of leaf nitrogen in rubisco (parameter FLNR in the model) to 0.0361 from 0.033. A lack of data exists to accurately parameterize FLNR (White et al., 2000), but the generally accepted range for this value for eastern deciduous broadleaf forests in using BIOME-BGC is between 0.033 and 0.2 (William M. Jolly, University of Montana, personal communication; Galina Churkina, Max-Planck Institute for Biogeochemistry, personal communication). Altering these two parameters led to a $\chi^2 = 0.28$, which showed no significant difference between the three observed metrics and our corresponding model output metrics.

In addition to calibrating BIOME-BGC to our site, it was also necessary to parameterize the model using atmospheric and landscape data. We synthesized historical atmospheric carbon dioxide trends using measurements from the Law Dome DE08 and DEO8-2 ice cores (1930–1957—Etheridge et al., 1998) and in situ air samples collected at Mauna Loa Observatory, Hawaii (1958–2006—Keeling et al., 2005). Nitrogen deposition values were based on the assumption that nitrogen emissions are representative of deposition. We used literature on national air quality and pollutants (EPA, 2000, 2003, 2007), EDGAR-HYDE 1.4 (Van Aardenne et al., 2001 adjusted to Olivier and Berdowski, 2001), and National Atmospheric Deposition Program grid data (NADP, 2008) to construct nitrogen deposition values from 1930 to 2006 using methods similar to Han (2007).

Daily climate data (i.e. daily precipitation and maximum and minimum temperature) were obtained from the National Climatic Data Center (NCDC). Nearest local station data (Ann Arbor, Dundee, Milan, Willis, and Ypsilanti, MI) were used to construct historical climate records from 1930 to 2006. We replaced NCDC observations with those obtained in the field for 2006 where available and used the MTCLIM model to produce daily values of short-wave radiation (W m^{-2}), vapour pressure deficit (Pa), average daylight temperature, and day length. Together these seven climatic variables along with year and year-day provided the climatic input to BIOME-BGC.

Forest cover data for Dundee Township 2001 were obtained from the National Land Cover Database (NLCD, Homer et al., 2007) at a resolution of 30 m. We reclassified the following NLCD land cover classes to forest: woody wetlands (1.9%, 2353.5 ha), mixed forest (0.15%, 182.7 ha), deciduous forest (8.4%, 10566.9 ha) and then resampled the data to a 15 m × 15 m cell size to correspond to our field measurements. From the resulting forest data layer, we created three grids that defined the distance each cell was from the east-, south-, and west-facing edge of the forest patch. Then we converted these edge orientation grids to a point vector file and spatially joined each edge-point file to obtain a single point file with the degree of edge for each cardinal direction for all forest grid cells in the township (a total of 58,400 points). Since BIOME-

Table 2
Existing literature describing carbon (C) and nitrogen (N) loss due to agricultural land use.

% C loss	% N loss	Sample *N*	Depth	Location	Forest type	Study type	# of literature sources	Source
43.4 (4.0)	–	14	A horizons	Global	All types	Review	7	Davidson and Ackerman (1993)
36.8 (3.7)	–	14	A and B horizons	Global	All types	Review	7	Davidson and Ackerman (1993)
31.5 (4.4)	–	18	A and B horizons	Global	All types	Review	8	Davidson and Ackerman (1993)
14.7 (7.2)	–	21	Entire solum	Global	All types	Review	5	Davidson and Ackerman (1993)
34.0 (4.4)	–	20	Fixed depth—top layer	Global	All types	Review	8	Davidson and Ackerman (1993)
26.2 (4.6)	–	25	Fixed depths >30 cm	Global	All types	Review	9	Davidson and Ackerman (1993)
25.9 (3.6)	–	55	All data	Global	All types	Review	18	Davidson and Ackerman (1993)
45.3 (5.9)	–	35	0–15 cm	Global	All types	Review	–	Murty et al. (2002)
19.2 (2.6)	–	27	0–45 cm	Global	All types	Review	–	Murty et al. (2002)
23.8 (3.0)	15.4 (3.5)	61	–	Global	All types	Review	–	Murty et al. (2002)
27 (4.6)	15.8 (5.5)	29	–	Global	All types	Review	–	Murty et al. (2002)
24	16	4	0–[23.0–39.5] cm	Bond Head, Ontario	Red pine, white pine	Research	–	Ellert and Gregorich (1996)
20	−17	4	0–[23.0–39.5] cm	C. Blondeau, Ontario	White pine	Research	–	Ellert and Gregorich (1996)
55	38	4	0–[23.0–39.5] cm	Delhi, Ontario	Maple, beech, white oak	Research	–	Ellert and Gregorich (1996)
68	33	4	0 [23.0–39.5] cm	Edwards, Ontario	Hemlock, white pine	Research	–	Ellert and Gregorich (1996)
38	12	4	0–[23.0–39.5] cm	Exeter, Ontario	Oak, ironwood	Research	–	Ellert and Gregorich (1996)
23	−7	4	0–[23.0–39.5] cm	Fonthill, Ontario	Red oak, white pine	Research	–	Ellert and Gregorich (1996)
8	−2	4	0–[23.0–39.5] cm	Highgate, Ontario	Maple, beech	Research	–	Ellert and Gregorich (1996)
4	−7	2	0–[23.0–39.5] cm	Kapuskasing, Ontario	Pine, black spruce	Research	–	Ellert and Gregorich (1996)
30	4	4	0–[23.0–39.5] cm	Kemptville, Ontario	Pine	Research	–	Ellert and Gregorich (1996)
24	15	4	0–[23.0–39.5] cm	Panmure, Ontario	Jack pine	Research	–	Ellert and Gregorich (1996)
40	26	4	0–[23.0–39.5] cm	Plainfield, Ontario	Maple, hemlock, beech	Research	–	Ellert and Gregorich (1996)
34	27	4	0–[23.0–39.5] cm	Ste. Anne, Ontario	Sugar maple	Research	–	Ellert and Gregorich (1996)
29	33	4	0–[23.0–39.5] cm	Vineland, Ontario	Cheery orchard	Research	–	Ellert and Gregorich (1996)
49	36	8	0–[23.0–39.5] cm	Winchester, Ontario	Maple, beech, white oak	Research	–	Ellert and Gregorich (1996)
47	43	4	0–[23.0–39.5] cm	Woodslee, Ontario	Shagbark hickory	Research	–	Ellert and Gregorich (1996)
34	19	66	0–[23.0–39.5] cm	All Sites	All types	Research	–	Ellert and Gregorich (1996)
9	–	537	Various depths	Global	All types	Review	74	Guo and Gifford (2002)
42	–	37	0–60 cm	Global	All types	Review	–	Guo and Gifford (2002)
40	–	469	0–15 cm	Global	All types	Review	50	Mann (1986)
26	–	212	15–30 cm	Global	All types	Review	50	Mann (1986)
42	–	86	30–45 cm	Global	All types	Review	50	Mann (1986)
26	–	274	0–30 cm	Global	All types	Review	50	Mann (1986)
29	8	625	0–15 cm	U.S. Locations	All types	Review	–	Post and Mann (1990)
22	4	625	0–30 cm	U.S. Locations	All types	Review	–	Post and Mann (1990)
23	6	625	0–100 cm	U.S. Locations	All types	Review	–	Post and Mann (1990)

(–) No available data reported. Standard error reported in parentheses for % C loss where available.

BGC also requires rooting depth, soil texture, elevation, and slope information for each location, we intersected our point layer with Soil Survey Geographic (SSURGO) soils data and Michigan Center for Geographic Information (MCGI) elevation and slope data. From SSURGO we acquired the rooting depth as the depth from the top of the A horizon to the bottom of the C horizon as well as soil texture characteristics (i.e. percent sand, silt, clay). Some of the NLCD-defined forest areas were removed from the analysis as they did not match soil delineations defined by SSURGO. For example, areas delineated as forest by NLCD and also as water, pits and quarries, and pits-aquents complex by SSURGO were removed from the analysis. This left 56,768 points remaining. The attribute table was then imported into XL-BGC, the Microsoft Excel version of BIOME-BGC. The equations, variables, and parameters in XL-BGC are virtually the same as in its Unix counterpart.

2.4. Computational experiments

2.4.1. Four temperature treatments

We developed four air-temperature treatments to apply within each of two modelling experiments to determine the effects of climate and patch heterogeneity on carbon pool and flux estimates. In the first treatment, we applied locally gathered NCDC air-temperature data to all forest locations. This treatment provided a reference for comparison for other treatments because it is typically NCDC data or data obtained from similar methods that are used by BIOME-BGC users.

In the second treatment, we used our field-based air-temperature data (daily minimum, maximum, and daylight average) collected external to the forest patch (year 2006). A correlation analysis between the external forest patch data and the reference data using a Pearson correlation coefficient statistic (0.859) and Levene's variance test ($p = 0.00$) showed that the external study patch and NCDC air-temperature data were significantly correlated and have similar variance at $\alpha = 0.05$. Given their high correlation, we applied the difference between field-based and reference air-temperature data from 2006 to the same year-day for historical data from 1930 to 2006.

The third treatment used our field-based air-temperature data collected in the forest patch interior. A high correlation coefficient statistic (0.881) between the interior forest patch and NCDC air-temperature data was also found, which allowed us to use the same method as above to alter historical temperature values for the third treatment. We refer to each of these three treatments as *reference temperature*, *exterior temperature*, and *interior temperature*, respectively. In each of these three air-temperature treatments the temperature across the landscape was homogeneous in that all locations received the same temperature.

Our fourth and last treatment was designed to be our best simulation of patch sizes, shapes, and edge effects in forest patches. Again, using the method described above, we altered the historical air-temperature data for each of the 5 edge zones measured for the east-, south-, and west-facing forest edge aspects as well as interior forest data (16 zones in total). In cases where an overlap existed between edge zones we applied a weighted mean of the temperature given by Eq. (2):

$$T_d = \frac{d_e \times t_e + d_s \times t_s + d_w \times t_w}{d_e + d_s + d_w} \tag{2}$$

where T_d is the edge distance weighted average temperature, d_e the edge zone weight of our temperature measurement from the east-facing edge where temperature T_e was taken, and correspondingly d_s and d_w are similar values for temperature measurements at t_s and t_w, respectively. When the distance of a cell was beyond 60 m from the east-, south-, and west-facing edges we used temperature data obtained from the forest interior. Effectively, this last scenario implements a heterogeneous air temperature across the landscape that can differentially affect local carbon storage and flux. We refer to this treatment hereafter as the *heterogeneous temperature treatment*.

2.4.2. Real landscape experiment

In the first modelling experiment, we quantified the effects of using each of the four different air-temperature treatments on forest carbon storage in the highly fragmented Dundee Township, Southeastern Michigan, using actual land cover (15 m resolution). The landscape characteristics of Dundee Township are heterogeneous, therefore our results were derived by running BIOME-BGC for each of 56,768 forest point locations that collectively formed 262 forest patches or 10% of the area of Dundee Township. We then scaled these results to the conterminous United States to provide an indication of the degree of influence edge effects could have on national carbon storage estimates.

2.4.3. Hypothetical landscape experiment

In our second experiment, we sought to generalize our results by reporting the sensitivity of carbon storage to variation in the spatial pattern of forest patches. Using hypothetical landscapes similar to those created by Franklin and Forman (1987), we created a ~992.25 ha (210 × 210 cell, 15 m resolution) landscape with 50% forest cover. We then altered the edge/area ratio metric of forest pattern to evaluate the effects of pattern on carbon storage. In each hypothetical landscape soil texture, slope, and elevation are homogeneous (Fig. 2).

Each simulation within each experiment consisted of a number of forest patch assumptions. For instance, patches were assumed to be homogeneous in age, height and density. Patch edges were defined as open (Matlack, 1993) and assumed to be adjacent to open fields or residential turf. For each simulation we report measurements of vegetation C, litter C, soil C, and total C at the end of 2006. Cell resolution in each experiment was 15 m (225 m^2) and the total area represented was 992.25 and 12,587 ha for the hypothetical and Dundee Township landscapes, respectively. We sum the results across all cells in the landscape for each treatment, and therefore our results report the aggregate outcome of each hypothetical landscape and Dundee Township after 77 years of forest growth.

3. Results

3.1. Analysis of field data

The estimated median temperature from a non-parametric Friedman test revealed a decrease in maximum temperature from the forest patch edge to a depth of 80 m (Fig. 3). Compared against critical χ^2 values at $\alpha = 0.01$ our computed χ^2 values (c.v. = 13.28 for each transect and 30.58 for all sensors) were substantially greater and provide evidence that temperature among measurement locations were significantly different within transects and among all sensors. Median ranks for the minimum temperatures are less prominent (Fig. 3) and therefore we focus the remainder of our discussion on maximum temperature.

The functional data analysis (described in Section 2.2) revealed an overall trend of decreasing maximum temperature from the forest edge inward. During daylight hours this trend existed for approximately 83%, 80%, and 94% of our measurements on the west, south, and east edges, respectively (Table 3).

In addition to illustrating the existence of air-temperature alterations from the forest patch edge to the patch interior, results show a switch near sunrise (i.e. ~6 a.m.) from a warmer interior and cooler exterior to the reverse. The east edge experienced a much greater warming in the morning when low sun angles were directed

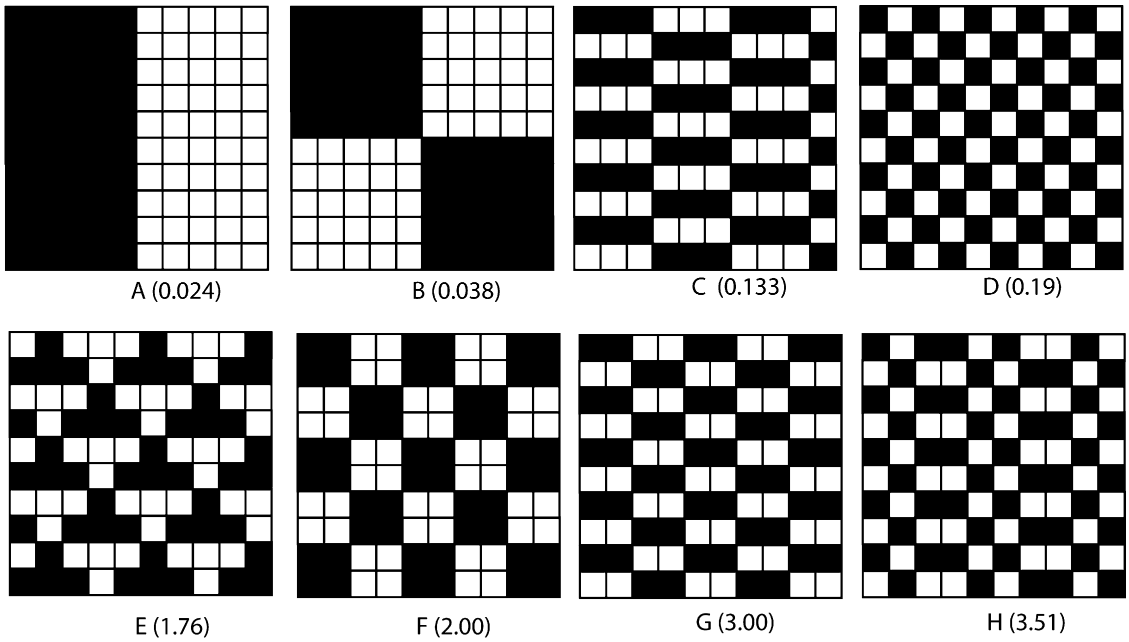

Fig. 2. Hypothetical landscape patterns. Values in parentheses denote edge/area ratio for landscape with illustrated pattern. (A)–(D) are complete landscapes with 50% forest. While all landscapes have a resolution of 15 m, each cell in (A)–(D) represents a collection of 21 × 21 cells and each cell in (E)–(H) are the individual 15 m^2 cells. At the aggregate level the patterns in (E)–(H) were not visible and therefore we had to zoom in on the landscape. White squares denote areas of forest, while black squares denote areas of no forest. Additional landscapes not shown here include complete fragmentation, i.e. alteration of forest non-forest for every cell (4.00), 3 × 3 cell blocks (0.67), 4 × 4 cell blocks (0.52), and 7 × 7 cell blocks (0.29).

Table 3
Summary statistics of functional analysis demonstrating the temperature gradient direction from forest patch edge to the patch interior. Negative slope (m) = cooler towards the interior, conversely $m > 0$ means it is warmer towards the interior; $m = 0$ means no gradient. T_{obs} = maximum temperature values observed.

	All T_{obs}			6 a.m. > T_{obs} > 6 p.m.			6 a.m. < T_{obs} < 6 p.m.		
	West	South	East	West	South	East	West	South	East
$m > 0$	28.17%	35.02%	33.97%	40.79%	55.68%	62.42%	15.54%	17.53%	5.53%
$m = 0$	4.21%	4.45%	5.29%	7.05%	7.26%	9.86%	1.36%	2.14%	0.72%
$m < 0$	67.59%	60.50%	60.66%	52.08%	37.06%	27.56%	82.93%	80.33%	93.67%

on the eastern patch edge. The warming of the east edge decreased near noon as the sun passed overhead, which then began to warm the western edge. The south-facing edge to interior air-temperature gradient was lower (i.e. less slope) but experienced increased persistence of edge effects from sunrise to sunset (data not shown).

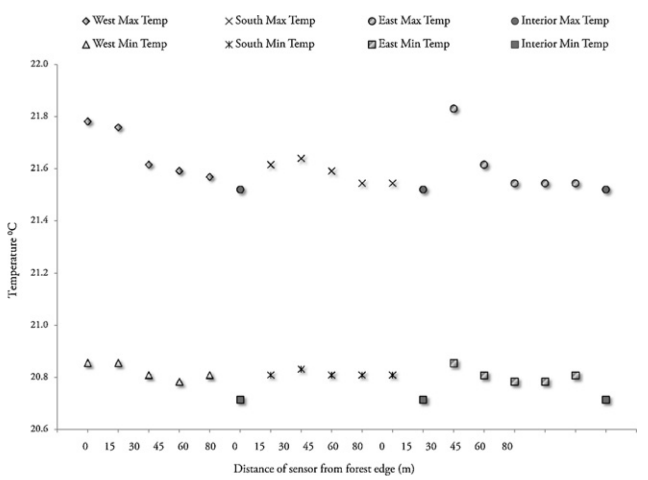

Fig. 3. Median values of maximum and minimum temperature for each sensor by distance from forest edge.

3.2. Analysis of Dundee Township carbon storage responses

Using BIOME-BGC we produced simulated measures of three carbon pools (kg C m^{-2}): vegetation, litter, and soil carbon. Vegetation C includes leaf, live coarse and fine root, live and dead stem carbon; litter carbon includes coarse woody debris (CWD) and litter carbon found in labile, unshielded cellulose, shielded cellulose, and lignin litter pools; soil carbon is the sum of carbon found in fast, medium, and slow microbial recycling pools in the mineral soil as well as that in recalcitrant soil organic matter (SOM) pool. The sum of the three pools provides a measure of total ecosystem carbon (Fig. 6).

Results from applying each of our four air-temperature treatments indicated a lower level of soil carbon for the reference treatment compared to the other treatments (Fig. 4). On average temperature values ranked from coolest to warmest were: reference, interior, heterogeneous, and exterior with the mean daily temperature value (°C) of each treatment over the 77 years as 9.20, 9.46, 9.65, and 10.02, respectively. Estimated levels of soil C followed: 127,437, 140,321, 141,903, and 148,422 Mg C, respectively. Therefore, growing forest across Dundee Township for 77 years under a 0.82 °C range of air temperature led to a difference of up to 20,985 Mg of soil carbon in the aggregate or 1.64 kg C m^{-2} of forest area. Assuming that the heterogeneous treatment provides the most realistic account of air-temperature conditions, relative to the output of soil C from the heterogeneous treatment, the interior treatment underestimated soil C by 1.24 Mg per ha and

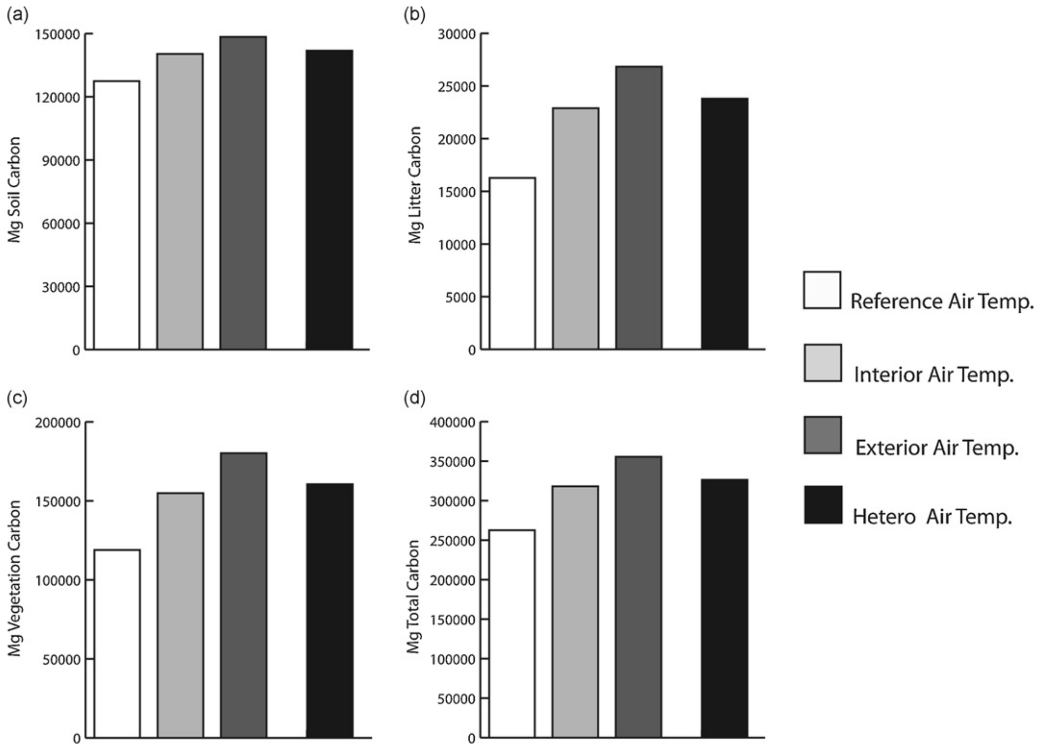

Fig. 4. Homogeneous vs. heterogeneous air-temperature treatments. Values represent total amount of carbon in soil (A), litter (B), vegetation (C), and all pools in total (D), as simulated, for all forest patches summed across Dundee Township under the real landscape experiment. Each of the Reference (climate data provided by the National Climate Data Center, NCDC), Interior (use of field data obtained within the interior of the forest patch), and Exterior Air Temp. (use of microclimate data obtained external to the forest patch) treatments are homogeneous in that the same climate was applied to all forested area in the township. The heterogeneous temperature treatment (Hetero Air Temp.) used field data obtained along transects from the forest patch edge to the interior on the east-, south-, and west-facing aspects.

the exterior treatment overestimated soil carbon by 5.1 Mg per ha.

Litter carbon, the smallest of the three carbon pools measured, experienced a range of 10 Mg of carbon difference among the air-temperature treatments. Again the exterior treatment produced the highest levels of litter carbon at 26,836 Mg for the entire township, followed by the heterogeneous treatment with 23,799 Mg, the interior treatment (22,892 Mg), and the reference treatment at 16,271 Mg C. Differences in litter carbon directly resulted from differences in vegetation carbon, which showed the same treatment ranking from highest to lowest.

Vegetation carbon pools were slightly larger than soil carbon pools, which is indicative of the distribution of above and below ground C in eastern deciduous forests near 40° latitude (Dixon et al., 1994). Vegetation C accounted for the majority of the carbon discrepancy among treatments with an overall range 61,280 Mg C among treatments. Values of 118,888, 160,570, 180,168, and 154,866 for each of the reference, heterogeneous, exterior, and interior treatments, respectively, illustrate the large difference between representing within-patch heterogeneity (i.e. ~6000 Mg C underestimation using interior treatment relative to the heterogeneous treatment and ~20,000 Mg C overestimation using the exterior treatment) versus homogeneous patch measurements. These vegetation C outputs corroborate theory and empirical work that illustrate the positive influence of increased temperature on vegetation growth when all other factors, such as soil water and nutrients, are not limiting (Lieth, 1975; Schlesinger, 1997). The difference in vegetation C was much larger than either of the soil or litter C pools, indicating that vegetation production in BIOME-BGC is much more sensitive to air temperature differences than is decomposition of soil carbon. The range of treatments led to a relative difference vegetation C of up to 4.80 kg C m^{-2} in forested areas.

Total estimated carbon storage for Dundee Township forest was 26,596, 318,079, 326,272, and 355,426 Mg C for each of the reference, interior, heterogeneous, and exterior air-temperature treatments. The larger estimates from field-based temperature treatments (55,483–92,830 Mg more) compared to that obtained by the reference treatment can be explained by increased vegetation growth due to higher the temperatures of the field-based treatments. The increased growth positively feeds back onto increased litter and soil C pools, which further facilitate vegetation growth. These results illustrate the influence of landscape heterogeneity on model results such that differences in temperature taken at a field study site versus some distance away may lead to discrepancies at the township level of 92,830 Mg C or 7.27 kg C m^{-2} in forested areas.

Our estimates of carbon storage in each pool are based on ~56,000 independent simulations that make up the forest cover in Dundee Township as illustrated in Fig. 5. While heterogeneous site characteristics did alter total C values across the township, because the reference, interior, and exterior treatments applied a homogeneous climate to the township, it was often the case that individual patches produced very similar levels of total carbon storage. In contrast the heterogeneous treatment produced varied carbon levels within the patch and among patches.

3.3. Analysis of carbon storage response to landscape fragmentation

Application of the 3 homogeneous air-temperature treatments to 12 hypothetical landscapes (Fig. 2), each with 50% forest but different edge/area ratio patterns, produced results similar to the Dundee Township experiment. Specifically, the largest estimate of carbon storage occurred using the exterior air-temperature treatment (13,986 Mg C) followed by the interior and reference treatments, 12,350 and 10,093 Mg C, respectively (Table 4). Because

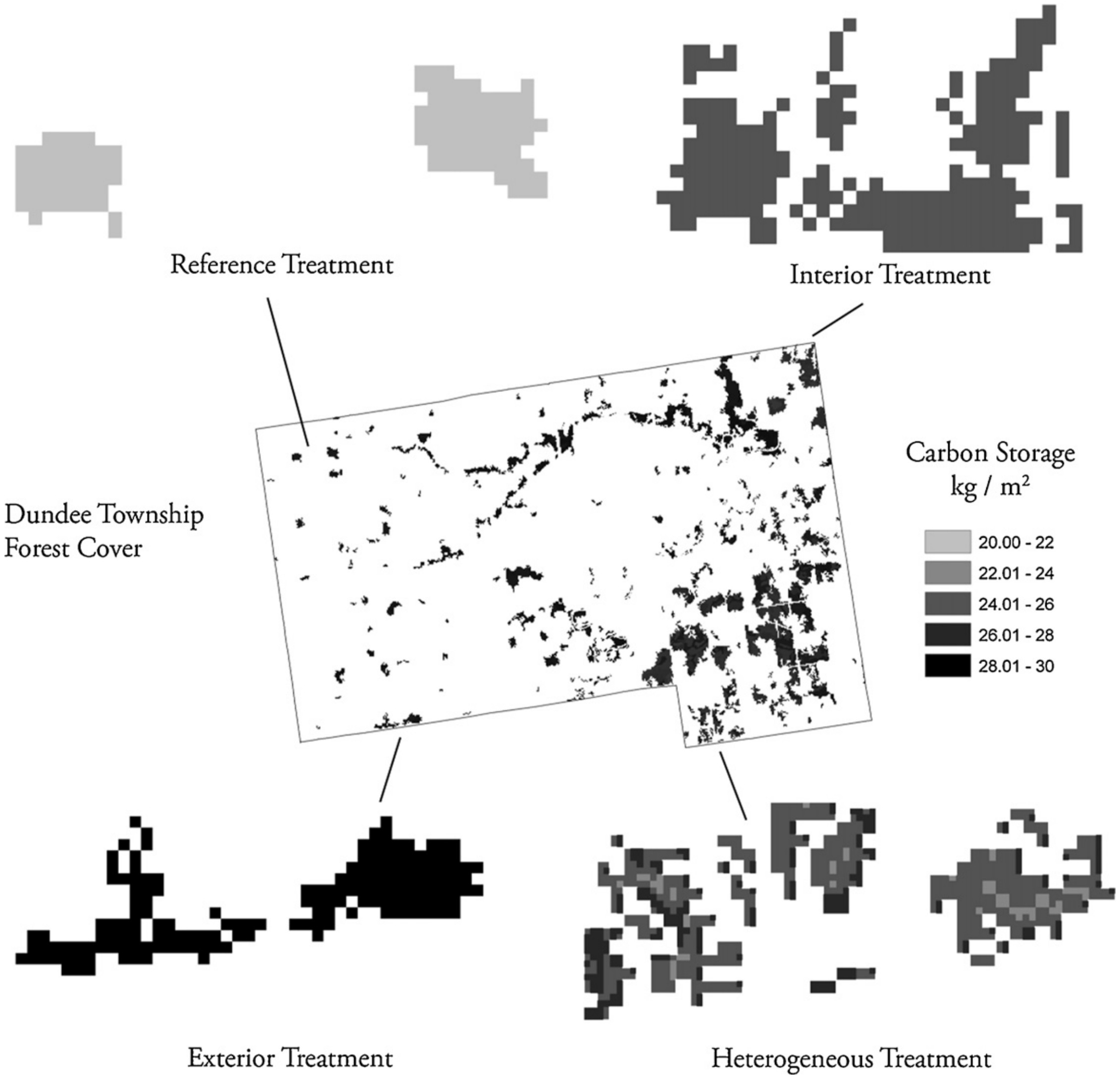

Fig. 5. Spatial distribution of deciduous forest in Dundee Township (center) and typical carbon storage output for different forest patches under the following four climate data treatments: reference (upper left), interior (upper right), exterior (lower left), and heterogeneous (lower right). Treatments are as described in previous figures and in Section 2.3 model simulations.

Table 4
Description of hypothetical fragmented landscape characteristics and associated carbon storage estimates. Cell edges and areas represent summed values across the hypothetical landscape.

Air-temperature treatment	Landscape description	Fig. 2	# cell edges	Forest area (# cells)	Edge/area (cells)	Edge/area ($m\,m^{-2}$)	Vegetation (Mg C)	Litter (Mg C)	Soil (Mg C)	Total (Mg C)
Heterogeneous	Parallel patches	A	630	22,050	0.03	0.002	6252.88	870.86	5269.55	12393.29
	2 large square patches	B	920	22,050	0.04	0.003	6248.74	870.10	5267.63	12386.47
	Large horizontal patches	C	2,936	22,050	0.13	0.009	6264.53	871.48	5275.35	12411.36
	10 × 10 cell patches	D	4,200	22,050	0.19	0.013	6356.31	886.11	5296.96	12539.38
	7 × 7 cell patches	–	6,300	22,050	0.29	0.019	6607.36	926.51	5375.55	12909.43
	4 × 4 cell patches	–	11,440	22,050	0.52	0.035	6741.99	950.71	5429.52	13122.22
	3 × 3 cell patches	–	14,700	22,050	0.67	0.044	6857.59	971.11	5477.23	13305.94
	T-shaped patches	E	38,723	22,050	1.76	0.117	6906.11	980.84	5501.57	13388.52
	2 × 2 cell patches	F	44,102	22,050	2.00	0.133	6925.70	982.92	5504.64	13413.27
	2 cell horizontal patches	G	66,150	22,050	3.00	0.200	6891.61	978.04	5494.33	13363.97
	–	H	77,282	22,050	3.50	0.234	6974.89	994.11	5533.89	13502.89
	Complete checkerboard	–	88,200	22,050	4.00	0.267	7056.60	1009.89	5572.70	13639.18
Exterior	All landscapes equal	–	–	–	–	–	7321.32	1033.35	5631.28	13985.95
Interior	All landscapes equal	–	–	–	–	–	6222.62	866.32	5261.06	12350.00
NCDC	All landscapes equal	–	–	–	–	–	4759.11	607.26	4726.57	10092.95

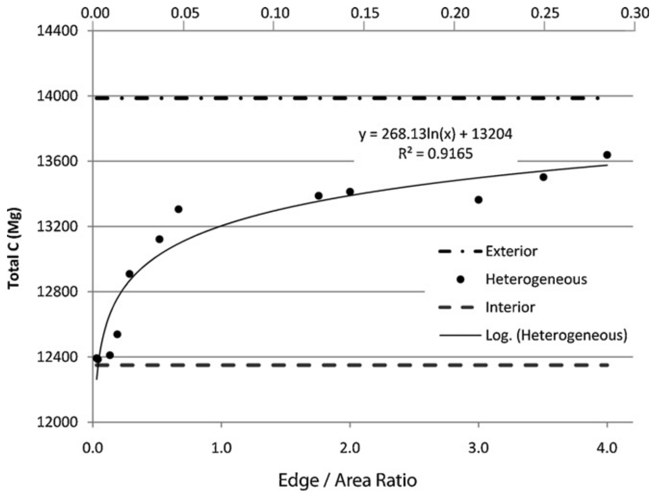

Fig. 6. Logarithmic increase in total carbon storage with landscape fragmentation as measured using the 12 hypothetical landscapes illustrated in Fig. 2 and described in Table 4. The upper x-axis displays edge/area ratio in units of meters (i.e. edge in meters/area in m^2) while the lower x-axis displays edge/area ratio in cell units (i.e. number of cell edges/number of cells). The logarithmic function is meters is $y = 267.7 \ln(x) + 13929$ ($r^2 = 0.92$).

we held the site conditions constant in this experiment, all 12 landscape patterns produced the same result in each of the three homogeneous air-temperature treatments.

In contrast to the homogeneous air-temperature treatments, the heterogeneous treatment results depended on the degree of fragmentation in the landscape. Specifically, as the landscape was altered from a single large patch to complete fragmentation (i.e. a checkerboard), carbon storage increased logarithmically to approximate the function $y = 268.13 \ln(x) + 13{,}204$, ($r^2 = 0.92$), where x is the ratio of total cell edge/total cell area across each hypothetical landscape. The logarithmic growth in carbon storage moved carbon estimates that closely aligned with the interior air-temperature treatment, when no fragmentation was present in the landscape, toward the exterior air-temperature treatment values when forest cover was completely fragmented (Fig. 6). Total carbon storage values show that fragmentation of a relatively unfragmented landscape (edge/area from 0 to 0.67) had more than three times the effect on carbon storage than did further fragmentation of a highly fragmented landscape (edge/area from 0.67 to 4 m m^{-2}; Table 4).

4. Discussion

4.1. Carbon responses

By back-casting the difference between each of our 2006 field-based treatments and the 2006 reference treatment to the years extending from 1930 to 2006 and simulating carbon storage values across Dundee Township we were able to evaluate the effects of within-patch and landscape heterogeneity in air temperature on carbon storage in a fragmented and human-dominated landscape. Specifically the interior, heterogeneous, and exterior treatments produced 318,080, 326,272, and 355,427 Mg C, respectively, in Dundee Township at the end of 2006. Therefore, within-patch air-temperature heterogeneity produced an 8000 Mg C difference from the interior treatment and nearly a 30,000 Mg C difference from the exterior treatment. Clearly the choice and application of field-based temperature measurements is an important decision given that the overall range of outcomes differed by ~38,000 Mg C, and if we include the influence of landscape heterogeneity by adding the results from our reference treatment extends the range of uncertainty to ~93,000 Mg C among treatments.

The range of uncertainty in our carbon estimates at the landscape scale is influenced by the relative difference among air-temperature measurements. Published climate data from nearby stations (i.e. the reference treatment) had the lowest maximum temperature compared to field-based measurements outside and inside the forest patch (i.e. exterior and interior treatments) in 75% and 32% of the measurements, respectively, out of the 228-day range of collected data. In the initial years of model output, results showed a higher level of estimated C accumulation in soil and litter for the reference treatment relative to the other treatments, corroborating theory that cool moist temperatures harbor increased soil C relative to warmer and dryer climates (Schlesinger, 1997). However, because the interior, heterogeneous, and exterior temperatures were greater than the reference data, and because in BIOME-BGC the vegetation C pools proved to be more responsive (in positive C aggradation) than the soil C pools (in reduced C accumulation due to increased decomposition), the overall carbon storage was larger for each of those three treatments in both experiments when compared to carbon storage values for the reference treatment. The positive feedbacks of biogeochemical and nutrient cycling continued to differentiate the treatments over time due to the different external climate forcings imposed by our temperature treatments.

Our temperature treatments contained various forms of heterogeneity and corresponding degrees of realism. While reference data were obtained from sources typically used by ecosystem modellers (e.g. National Weather Service stations), station measurements can be poorly sited such that they are influenced by shadowing, humidity, isolation from wind, and other factors (Davey and Pielke, 2005; Peterson, 2006). Furthermore, station measurements can be inhomogeneous overtime and require adjustment due to station relocation, equipment change, and land-use and land-cover change (Karl and Williams, 1987; Pielke et al., 2007b). Post-experiment investigation of why our reference treatment held lower values than the field-based measurements revealed that the Dundee NWS station was located in the middle of a wastewater treatment plant. Not only was the station surrounded by open liquid waste treatment pools but also the treatment plant was within proximity to a river on three sides. The result was a station location that experienced a very local microclimate that had substantially greater humidity then locations less than half a kilometer away. Assuming all climate and radiation conditions are equal, increased humidity will lead to a reduction in the surface air temperature (Pielke et al., 2007a), explaining why our reference treatment had lower temperature values.

Using hypothetical landscapes, similar to those developed by Franklin and Forman (1987) to explore the general ecological consequences of fragmentation and by Smithwick et al. (2003) who investigated the effects of wind and light on forest patch carbon storage, we evaluated the effects of within-patch air-temperature heterogeneity on carbon storage in a number of fragmented landscapes. The logarithmic response of carbon storage to fragmentation suggests that under low fragmented landscapes interior forest air-temperature measurements may provide a closer approximation of air-temperature conditions within large forest patches than measurements taken exterior to the patch or typically acquired from NCDC or National Weather Service Stations. Conversely, in a highly fragmented landscape, air-temperature measurements taken exterior to the forest are more representative than those taken interior (Fig. 6). While our results corroborate theory and empirical work that demonstrate increased productivity with increased temperature (Lieth, 1975; Schlesinger, 1997), our modelling analysis does not take into account the effects of the following on carbon storage along or within edge zones: mortality and carbon removal along edge (e.g. by adjacent streams; Malanson and Kupfer, 1993), wind throw and light penetration (Smithwick et al., 2003), harvest and fire disturbance regimes (Smithwick et al., 2007), varying species composition or invasive species in edge habitats, or soil organic carbon changes due to land use and erosion (Yadav and Malanson, 2008). These processes could alter our results and are important topics for future research, but are beyond the scope of this paper.

4.2. Does the incorporation of edge effects influence forest patch carbon storage?

Our analyses of both real and hypothetical fragmented landscapes showed that within the range of observed temperature values and their corresponding MTCLIM climatic variable values, the BIOME-BGC carbon cycling processes and forest ecosystem carbon budgets were highly sensitive to edge effects. Under the real landscape experiment, the heterogeneous treatment (i.e. including edge effects) produced an overall ecosystem carbon storage value of 326,272 Mg C or an average of 25.55 kg C m^{-2}. Under the same experiment, using the less realistic homogeneous climate treatments, the interior and exterior treatments produced 318,080 Mg C (24.91 kg C m^{-2} on average) and 355,427 Mg C (27.83 kg C m^{-2} on average). Therefore basing carbon storage assessments on interior forest microclimate measurements could underestimate values by 0.64 kg C m^{-2}. More likely is the case that researchers using ecosystem biogeochemistry models like BIOME-BGC use climate measurements made in nearby open fields or at meteorological stations, in which case our analysis shows a large overestimation of 2.28 kg C m^{-2} on average.

Our results are significant because attempts to account for carbon uptake and storage in temperate forests have been necessary as part of the ongoing and broader effort to (a) close the carbon budget and account for the temperate carbon sink, and to (b) include more realistic representations of the effects of people on landscapes into ecosystem process models. By scaling up our average C storage values to the continental United States we can obtain an idea of the relative effect that within-patch heterogeneity could have on national carbon accounting. For example, using the 2001 National Land Cover Dataset (Homer et al., 2007) we found that the interior, heterogeneous, and exterior treatments produced 23.15, 23.75, and 25.89 Pg of total carbon storage, respectively, for deciduous forests across the United States. Despite the obvious and important simplifications involved in this scaling exercise, these results suggest that choosing a homogeneous representation of forest microclimate could underestimate carbon values by 0.6 Pg when interior forest measurements are used or overestimate carbon storage values by 2.14 Pg when temperature measurements are collected exterior to the forest patch. The range of over- and under-estimates pose a serious question about the degree to which within-patch heterogeneities influence carbon storage estimates since these differences among our modelling treatments are on the order of current estimates of the North American carbon sink (~1.7 Pg C yr^{-1} in the 1990s, Fan et al., 1998; ~0.65 Pg C yr^{-1} from 2000 to 2005, Peters et al., 2007; ~0.505 Pg, CCSP, 2007). Clearly within-patch heterogeneity at the micro level has an influence on the macro-level patterns of carbon storage across the United States. How we go about collecting data on within-patch heterogeneity at national and global scales and incorporating those data into national and global estimates of carbon storage remains a significant future endeavor.

Another significant feature of our results is in its implication for the use of vegetation process models to couple to regional or global climate models. We found that including patch heterogeneity tended to increase C accumulation and storage in forest patches as a result of increased forest production as simulated by BIOME-BGC. If patch heterogeneity does drive higher forest production per unit area, this would be reflected in larger leaf area, altering the canopy reflectance of short-wave radiation and the transfer of water vapour to the atmosphere through evapotranspiration.

4.3. Ecosystem processes in land-change models

By loosely integrating BIOME-BGC with a commercial GIS package we were able to (1) facilitate the retrieval of site characteristic data for running the model, and (2) visualize results of ecosystem function metrics spatially. A tight integration would allow us to apply BIOME-BGC at a high resolution and in a highly fragmented environment where multiple runs of the model may be conducted to alter the detail of landscape data (i.e. reducing the number of runs by running the model on polygon attributes or the converse by running the model on more detailed point data) or to alter the landscape to assess land-use and land-cover change scenarios. Contemporary research coupling human and environment systems for integrated assessments of land-use and land-cover change (LUCC) have linked agent-based models (ABMs) and GIS to evaluate the effects of land-use policies on forest cover (e.g. Robinson and Brown, in press). The combined use of a dynamic agent-based approach with ecosystem process models can help us better understand (a) the coupled human–environment processes that influence ecosystem function in fragmented and human-dominated, (b) the effects current and future landscape trends may have on ecosystem function and productivity as well as surface–atmosphere coupling, (c) the effects of policy and management decisions on landscape structure and function have and could have on ecosystem function, and (d) how changes and knowledge of ecosystem function and services could feedback to influence land-use and land-cover change decisions and trajectories.

5. Conclusions and future research

Simulation of ecosystem carbon cycling using the widely used biogeochemical process model BIOME-BGC in a heterogeneous, fragmented, and human-dominated landscape, combined with field-measured microclimate temperature patterns, showed that within-patch and landscape level heterogeneity and landscape fragmentation had a strong effect on ecosystem simulated carbon storage in the landscape. Simulated forest productivity and carbon storage were underestimated when temperature data from a National Weather Service maintained station were used and overestimated when field measured temperature data were used, in comparison to the more realistic simulations of the fragmented landscape using microclimatic temperature differences.

Our combined field and modelling study clearly demonstrated that simulated values for carbon cycling and ecosystem carbon stocks are highly sensitive to realistic patterns of forest fragmentation. Therefore as we improve our carbon estimating procedures, we need to include measurements of both within-patch and landscape heterogeneity and make strides to also incorporate human behaviors through land-use and land-cover change. Future research that identifies all permutations of fragmentation associated with different edge/area ratios may be able to provide insight for the creation of ranges of uncertainty associated with past and future carbon estimates. Similarly, statistics or indices of landscape heterogeneity may also prove to be useful in this endeavor.

The integration of biophysical models with land-use models allows for the identification of processes causing critical changes in ecosystem functions and the landscape patterns that act at different scales and are linked across scale. By quantifying the influence of human systems on ecosystems and how those ecosystems feedback we can better define (1) the impacts of humans on ecological systems, (2) the resilience and robustness of ecological systems to human-induced perturbations, and (3) the thresholds that result in ecosystem failure or decrease ecosystem function beyond their use to humans (Moran et al., 2005). Furthermore, if coupled with LUCC models of anthropogenic behavior, the representation of ecological outcomes by ecosystem process models can be used to quantify the effects of anthropogenic systems on the quality and functions of ecosystems (land-cover) and how those changes feedback to alter anthropogenic behavior. A tight integration of LUCC and ecosystem modelling approaches is the focus of novel research in these fields (Yadav et al., 2008).

Acknowledgements

Support for the presented research in the form of grants was provided by the National Science and Engineering Research Council of Canada (NSERC), the Graham Environmental Sustainability Institute (GESI) at the University of Michigan, and the National Science Foundation Biocomplexity in the Environment Program (BCS-0119804 and GEO-0814542) for Project SLUCE. We would also like to acknowledge with gratitude the intellectual support of our colleagues Leslie Sefsick, John S. Kimball, Rick Riolo, Scott Page, Donald R. Zak, Jason Taylor, Jose Garcia, Dan Bamber, Leslie Garrison, Greg Jacobs, Andrew Bell, Tingting Zhao, Haejin (Jinny) Han, Neil Carter, Jonathan Redmond, and Peter Johnson. Lastly, the authors would like to thank the anonymous reviewers and journal editor for their constructive comments.

References

Albert, D.A., 1995. Regional Landscape Ecosystems of Michigan, Minnesota, and Wisconsin: A Working Map and Classification, Gen. Tech. Rep. NC-178. U.S. Department of Agriculture, Forest Service, North Central Forest Experiment Station. Jamestown, ND: Northern Prairie Wildlife Research Center Online. http://www.npwrc.usgs.gov/resource/habitat/rlandscp/index.htm (Version 03JUN1998).

Arnfield, A.J., 2003. Two decades of urban climate research: a review of turbulence, exchanges of energy and water, and the urban heat island. Int. J. Climatol. 23, 1–26.

Barford, C.C., Wofsy, S.C., Goulden, M.L., Munger, J.W., Pyle, E.H., Urbanski, S.P., Hutyra, L., Saleska, S.R., Fitzjarrald, D., Moore, K., 2001. Factors controlling long- and short-term sequestration of atmospheric CO_2 in a mid-latitude forest. Science 294, 1688–1691.

Bolstad, P.V., Vose, J.M., McNulty, S.G., 2001. Forest productivity, leaf area, and terrain in Southern Appalachian deciduous forests. For. Sci. 47, 419–427.

Botkin, D.B., Simpson, L.G., Nisbet, R.A., 1993. Biomass and carbon storage of the North American deciduous forest. Biogeochemistry 20, 1–17.

Betts, A.K., Ball, J.H., Beljaars, A.C.M., Miller, M.J., Viterbo, P.A., 1996. The land surface-atmosphere interaction: A review based on observational and global modeling perspectives. J. Geophys. Res. 101, 7209–7225.

Cadenasso, M.L., Traynor, M.M., Pickett, S.T.A., 1997. Functional location of forest edges: gradients of multiple physical factors. Can. J. For. Res. 27, 774–782.

Caspersen, J.P., Pacala, S.W., Jenkins, J.C., Hurtt, G.C., Moorcroft, P.R., Birdsey, R.A., 2000. Contribution of land-use history to carbon accumulation in U.S. forests. Science 290, 1148–1151.

CCSP, 2007. The First State of the Carbon Cycle Report (SOCCR): The North American Carbon Budget and Implications for the Global Carbon Cycle. In: King, A.W., Dilling, L., Zimmerman, G.P., Fairman, D.M., Houghton, R.A., Marland, G., Rose, A.Z. and Wilbanks, T.J. (Eds.), A Report by the U.S. Climate Change Science Program and the Subcommittee on Global Change Research. National Oceanic and Atmospheric Administration, National Climatic Data Center, Asheville, NC, USA, 242 pp.

Chen, J., Franklin, J.F., Spies, T.A., 1995. Growing-season microclimatic gradients from clearcut edges into old-growth Douglas-fir forests. Ecol. Appl. 5, 74–86.

Clark III, A., Phillips, D.R., Frederick, D.J., 1986a. Weight, volume and physical properties of major hardwood species in the Piedmont. USDA Forest Service Tech. Rpt. SE-255.

Clark III, A., Phillips, D.R., Frederick, D.J., 1986b. Weight, volume and physical properties of major hardwood species in the Upland-South. USDA Forest Service Tech. Rpt. SE-257.

Collinge, S.K., 1996. Ecological consequences of habitat fragmentation: implications for landscape architecture and planning. Landsc. Urban Plann. 36, 59–77.

Coops, N.C., Waring, R.H., 2001. The use of multiscale remote sensing imagery to derive regional estimates of forest growth capacity using 3-PGS. Remote Sens. Environ. 75, 324–334.

Currie, W.S., Yanai, R.D., Piatek, K.B., Prescott, C.E., Goodale, C.L., 2003. Processes affecting carbon storage in the forest floor and in downed woody debris. In: Kimble, J.M., Heath, L.S., Birdsey, R.A., Lal, R. (Eds.), The Potential of U.S. Forest Soils to Sequester Carbon and Mitigate the Greenhouse Effect. CRC Press, Boca Raton, FL, pp. 135–157.

Curtis, P.S., Hanson, P.J., Bolstad, P., Barford, C.C., Randolph, J.C., Schmid, H.P., Wilson, K.B., 2002. Biometric and eddy-covariance based estimates of annual carbon storage in five eastern North American deciduous forests. Agric. For. Meterol. 113, 3–19.

Davey, C.A., Pielke Sr., R.A., 2005. Microclimate exposures of surface-based weather stations. Bull. Am. Meteorol. Soc. 86, 497–504.

Davidson, E.A., Ackerman, I.L., 1993. Changes in soil carbon inventories following cultivation of previously untilled soils. Biogeochemistry 20, 161–193.

Deadman, P.J., Robinson, D.T., Moran, E., Brondizio, E., 2004. Colonist household decisionmaking and land-use change in the Amazon Rainforest: an agent-based simulation. Environ. Plan. B 31, 693–709.

Dixon, R.K., Brown, S., Houghton, R.A., Solomon, A.M., Trexler, M.C., Wisniewski, J., 1994. Carbon pools and flux of global forest ecosystems. Science 263, 185–190.

Ellert, B.H., Gregorich, E.G., 1996. Storage of carbon, nitrogen and phosphorus in cultivated and adjacent forested soils of Ontario. Soil Sci. 161, 587–603.

EPA, 2000. National Air Pollutant Emission Trends, 1900–1998. United States Environmental Protection Agency, Office of Air Quality Planning and Standards. Research Triangle Park, NC 27711.

EPA, 2003. National Air Quality and Emissions Trends Report. United States Environmental Protection Agency, Office of Air Quality Planning and Standards. Research Triangle Park, NC 27711.

EPA, 2007. Latest Findings on National Air Quality. United States Environmental Protection Agency, Office of Air Quality Planning and Standards. Research Triangle Park, NC 27711.

Etheridge, D.M., Steele, L.P., Langenfelds, R.L., Francey, R.J., Barnola, J.M., Morgan, V.I., 1998. Historical CO_2 Record Derived from a Spline Fit (75 Year Cutoff) of the Law Dome DSS, DE08, and DE08-2 Ice Cores. Division of Atmospheric Research, CSIRO, Aspendale, Victoria, Australia. Laboratoire of Glaciologie et Geophysique de l'Environnement, Saint Martin d'Heres-Cedex, France. Antarctic CRC and Australian Antarctic Division, Hobart, Tasmania, Australia. http://www.cdiac.ornl.gov/ftp/trends/co2/lawdome.smoothed.yr75 (last viewed February 2008).

Fan, S., Gloor, M., Mahlman, J., Pacala, S., Sarmiento, J., Takahashi, T., Tans, P., 1998. A large terrestrial carbon sink in North America implied by atmospheric and oceanic carbon dioxide data and models. Science 282, 442–446.

Foley, J.A., DeFries, R., Asner, G.P., Barford, C.C., Bonan, G., Carpenter, S.R., Chapin, F.S., Coe, M.T., Daily, G.C., Gibbs, H.K., Helkowski, J.H., Holloway, T., Howard, E.A., Kucharik, C.J., Monfreda, C., Patz, J.A., Prentice, I.C., Ramankutty, N., Snyder, P.K., 2005. Global consequences of land use. Science 309, 570–574.

Franklin, J.F., Forman, R.T.T., 1987. Creating landscape patterns by forest cutting: ecological consequences and principles. Landsc. Ecol. 1, 5–18.

Frelich, L.E., 2002. Forest Dynamics and Disturbance Regimes. Studies from Temperate Evergreen-Deciduous Forests. Cambridge University Press, Cambridge, UK, 266 pp.

Gimblett, R.H., 2002. Integrating Geographic Information Systems and Agent-Based Modeling Techniques for Simulating Social and Ecological Processes. Oxford University Press, New York, 327 pp.

GLP, 2005. Global Land Project science plan and implementation strategy. IGBP Report No. 53/IHDP Report No. 19. IGBP Secretariat, Stockholm. 64 pp.

Gower, S.T., 2003. Patterns and mechanisms of the forest carbon cycle. Annu. Rev. Environ. Resour. 28, 169–204.

Guo, L.B., Gifford, R.M., 2002. Soil carbon stocks and land use change: a meta analysis. Global Change Biol. 8, 345–360.

Gustafson, E.J., Shifley, S.R., Mladenoff, D.J., Nimerfro, K.K., He, H.S., 2000. Spatial simulation of forest succession and timber harvesting using LANDIS. Can. J. For. Res. 30, 32–43.

Gutman, G., Janetos, A.C., Justice, C.O., Moran, E.F., Mustard, J.F., Rindfuss, R.R., Skole, D., Turner II, B.L., Cochran, M., 2004. Land Change Science: Observing, Monitoring and Understanding Trajectories of Change on the Earth's Surface. Remote Sensing and Digital Image Processing Series 6. Springer-Verlag, Berlin, 461 pp.

Han, H., 2007. Nutrient Loading to Lake Michigan: A Mass Balance Assessment. PhD Thesis. University of Michigan, Ann Arbor, MI.

He, H.S., Mladenoff, D.J., Boeder, J., 1999a. An object-oriented forest landscape model and its representation of tree species. Ecol. Model. 119, 1–19.

He, H.S., Mladenoff, D.J., Crow, T.R., 1999b. Linking an ecosystem model and a landscape model to study forest species response to climate warming. Ecol. Model. 114, 213–233.

Homer, C., Dewitz, J., Fry, J., Coan, M., Hossain, N., Larson, C., Herold, N., McKerrow, A., VanDriel, J.N., Wickham, J., 2007. Completion of the 2001 national land cover database for the conterminous United States. Photogramm. Eng. Remote Sens. 73, 337–341.

Houghton, R.A., Hackler, J.L., Lawrence, K.T., 1999. The U.S. carbon budget: contributions from land-use change. Science 285, 574–578.

Howe, E., Baker, W.L., 2003. Landscape heterogeneity and disturbance interactions in a subalpine watershet in Northern Colorado, USA. Ann. Assoc. Am. Geogr. 93, 797–813.

Hubacek, K., Vazquez, J., 2002. The Economics of Land Use Change No. IR-02-015. International Institute for Applied Systems Analysis, Laxenburg, Austria.

Huigen, M.G.A., 2004. First principles of the MameLuke multi-actor modelling framework for land use change, illustrated with a Philippine case study. J. Environ. Manage. 72, 5–21.

Jeltsch, F., Milton, S., Dean, W.R.J., van Rooyen, N., 1996. Tree spacing and coexistence in semiarid Savannas. J. Ecol. 84, 583–595.

Jung, M., Le Maire, G., Zaehle, S., Luyssaert, S., Vetter, M., Churkina, G., Ciais, P., Viovy, N., Reichstein, M., 2007. Assessing the ability of three land ecosystem models to

simulate gross carbon uptake of forests from boreal to Mediterranean climate in Europe. Biogeosciences 4, 647–656.
Karl, T.R., Williams Jr., C.N., 1987. An approach to adjusting climatological time series for discontinuous inhomogeneities. J. Clim. Appl. Meteorol. 26, 1744–1763.
Keeling, C.D., Whorf, T.P., Group, C.D.R., 2005. Atmospheric CO_2 Concentrations (ppmv) Derived From In Situ Air Samples Collected at Mauna Loa Observatory, Hawaii. Scripps Institution of Oceanography (SIO), University of California, La Jolla, California 92093-0444, USA.
Lambin, E.F., Baulies, X., Bockstael, N., Fischer, G., Krug, T., Leemans, R., Moran, E.F., Rindfuss, R.R., Sato, Y., Skole, D., Turner II, B.L., Vogel, C., 1999. Land-Use and land-Cover Change: Implementation Strategy, International Geosphere-Biosphere Programme (IGBP) Report 48 and the International Human Dimensions Programme on Global Environmental Change (IHDP) Report 10. IGBP Secretariat, Royal Swedish Academy of Science, Stockholm.
Landsberg, H.E., 1970. Man-made climatic changes. Science 170, 1265–1274.
LI-COR, 1992. LAI-2000 Plant Canopy Analyzer Operating Manual. LI-COR Inc., Box 4425/4421 Superior St., Lincoln, Nebraska 68504, USA.
Lieth, H., 1975. Modeling the primary productivity of the world. In: Lieth, H., Whittaker, R.H. (Eds.), Primary Productivity of the Biosphere. Springer-Verlag, New York, pp. 237–263.
Lobo, J., 2004. Bringing cities into complexity science. SFI Bull. (Winter), 8–9.
Malanson, G.P., Kupfer, J.A., 1993. Simulated fate of leaf litter and large woody debris at a riparian cutbank. Can. J. For. Res. 23, 582–590.
Mann, L.K., 1986. Changes in soil carbon storage after cultivation. Soil Sci. 142, 279–288.
Matlack, G.R., 1993. Microenvironment variation within and among forest edge sites in the eastern United States. Biol. Conserv. 66, 185–194.
Moran, E., Ojima, D., Buchmann, N., Canadell, J., Coomes, O., Graumlich, L., Jackson, R., Jaramillo, V., Lavorel, S., Leadley, P., Matson, P., Murdiyarso, D., Porter, J., Pfaff, A., Pitelka, L., Rajan, K., Ramankutty, N., Turner II, B., Yagi, K., 2005. Global Land Project: Science Plan and Implementation Strategy, IGBP Report No. 53/IHDP Report No. 19, IGBP Secretariat.
Murty, D., Kirschbaum, M.U.F., McMurtie, R.E., McGilvray, H., 2002. Does conversion of forest to agricultural land change soil carbon and nitrogen? A review of the literature. Global Change Biol. 8, 105–123.
NADP, 2008. National Atmospheric Deposition Program (NRSP-3). NADP Program Office, Illinois State Water Survey, 2204 Griffith Dr., Champaign, IL 61820.
Newman, G.S., Arthur, M.A., Muller, R.N., 2006. Above- and belowground net primary production in a temperate mixed deciduous forest. Ecosystems 9, 317–329.
Olivier, J.G.J., Berdowski, J.J.M., 2001. Global emissions sources and sinks. In: Berdowski, J., Guicherit, R., Heij, B.J. (Eds.), The Climate System. A.A. Balkema Publishers/Swets & Zeitlinger Publishers, Lisse, Netherlands, pp. 33–78.
Parker, D.C., Berger, T., Manson, S., et al., 2002. Agent-Based Models of Land-Use and Land-Cover Change. Report and Review of an International Workshop. LUCC Focus 1 Office, Anthropological Center for Training and Research on Global Environmental Change Indiana University, Irvine, California, USA, October 4–7, 2001.
Parton, W.J., Schimel, D.S., Cole, C.V., Ojima, D.S., 1987. Analysis of factors controlling soil organic matter levels in great plains grasslands. Soil Sci. Soc. Am. J. 51, 1173–1179.
Peters, W., Jacobson, A.R., Sweeney, C., Andrews, A.E., Conway, T.J., Masarie, K., Miller, J.B., Bruhwiler, L.M.P., Petron, G., Hirsch, A.I., Worthy, D.E., van der Werf, G.R., Randerson, J.T., Wennberg, P.O., Krol, M.C., Tans, P.P., 2007. An atmospheric perspective on North American carbon dioxide exchange: CarbonTracker. Proc. Natl. Acad. Sci. 104, 18925–18930.
Peterson, T.C., 2006. Examination of potential biases in air temperature caused by poor station locations. Bull. Am. Meteorol. Soc. 87, 1073–1080.
Pielke Sr., R.A., Davey, C.A., Niyogi, D., Fall, S., Steinweg-Woods, J., Hubbard, K., Lin, X., Cai, M., Lim, Y.-K., Li, H., Nielsen-Gammon, J., Gallo, K., Hale, R., Mahmood, R., Foster, S., McNider, R.T., Blanken, P., 2007a. Unresolved issues with the assessment of multidecadal global land surface temperature trends. J. Geophys. Res. 112, D24S08, doi:10.1029/2006JD008229.
Pielke Sr., R.A., Marland, G., Betts, R.A., Chase, T.N., Eastman, J.L., Niles, J.O., Niyogi, D.D.S., Running, S.W., 2002. The influence of land-use change and landscape dynamics on the climate system: relevance to climate-change policy beyond radiative effect of greenhouse gases. Philos. Trans. R. Soc. Lond. Ser. A 360, 1705–1719.
Pielke Sr., R.A., Nielsen-Gammon, J., Davey, C., Angel, J., Bliss, O., Doesken, N., Cai, M., Fall, S., Niyogi, D., Gallo, K., Hale, R., Hubbard, K.G., Lin, X., Li, H., Raman, S., 2007b. Documentation of uncertainties and biases associated with surface temperature measurement sites for climate change assessment. Bull. Am. Meteorol. Soc. 88, 913–928.
Poschlod, P., Bakker, J.P., Kahmen, S., 2005. Changing land use and its impact on biodiversity. Basic Appl. Ecol. 6, 93–98.
Post, W.M., Mann, L.K., 1990. Changes in soil organic carbon and nitrogen as a result of cultivation. In: Bouwman, A.F. (Ed.), Soils and Greenhouse Effect. Wiley, New York, pp. 401–406.
Raddatz, R.L., 2007. Evidence for the influence of agriculture on weather and climate through the transformation and management of vegetation: illustrated by examples from the Canadian prairies. Agric. For. Meteorol. 142, 186–202.
Riebsame, W.E., Meyer, W.B., Turner II, B.L., 1994. Modeling land use and cover as part of global environmental change. Clim. Change 28, 45–64.
Robinson, D.T., Brown, D.G., in press. Evaluating the effects of land-use development policies on ex-urban forest cover: an integrated agent-based GIS approach. Int. J. Geogr. Inform. Sci.
Rosenberg, N.J., Blad, B.L., Verma, S.B., 1983. Microclimate: The Biological Environment. Wiley, New York, 495 pp.
Running, S.W., Coughlan, J.C., 1988. A general model of forest ecosystem processes for regional applications. 1. Hydrologic balance, canopy gas exchange and primary production processes. Ecol. Model. 42, 125–154.
Running, S.W., Hunt, R.E., 1993. Generalization of a forest ecosystem process model for other biomes, BIOME-BGC, and an application for global-scale models. In: Ehleringer, J.R., Field, C.B. (Eds.), Scaling Physiological Processes: Leaf to Globe. Academic Press Inc., pp. 141–158.
Running, S.W., Nemani, R.R., Hungerford, R.D., 1987. Extrapolation of synoptic meteorological data in mountainous terrain and its use for simulating forest evapotranspiration and photosynthesis. Can. J. For. Res. 17, 472–483.
Schimel, D., Melillo, J., Tian, H., McGuire, A.D., Kicklighter, D.W., Kittel, T., Rosenbloom, N., Running, S., Thornton, P., Ojima, D., Parton, W., Kelly, R., Sykes, M., Neilson, R., Rizzo, B., 2000. Contribution of increasing CO_2 and climate to carbon storage by ecosystems in the United States. Science 287, 2004–2006.
Schlesinger, W.H., 1997. Biogeochemistry: An Analysis of Global Change. Academic Press, San Diego, CA, 588 pp.
Sheskin, D., 2004. Handbook of Parametric and Nonparametric Statistical Procedures. Chapman & Hall/CRC, Boca Raton, FL, 1193 pp.
Shugart, H.H., 2000. Importance of structure in the longer-term dynamics of landscapes. J. Geophys. Res. (D Atmos.) 105, 20065–20075.
Smithwick, E.A.H., Harmon, M.E., Domingo, J.B., 2003. Modeling multiscale effects of light limitations and edge-induced mortality on carbon stores in forest landscapes. Landsc. Ecol. 18, 701–721.
Smithwick, E.A.H., Harmon, M.E., Domingo, J.B., 2007. Changing temporal patterns of forest carbon stores and net ecosystem carbon balance: the stand to landscape transformation. Landsc. Ecol. 22, 77–94.
Tatarinov, F.A., Cienciala, E., 2006. Application of BIOME-BGC model to managed forests. 1. Sensitivity analysis. For. Ecol. Manage. 237, 267–279.
Ter-Mikaelian, M.T., Korzukhin, M.D., 1997. Biomass equations for sixty-five North American tree species. For. Ecol. Manage. 97, 1–24.
Thornton, P.E., Law, B.E., Gholz, H.L., Clark, K.L., Falge, E., Ellsworth, D.S., Goldstein, A.H., Monson, R.K., Hollinger, D., Falk, M., Chen, J., Sparks, J.P., 2002. Modeling and measuring the effects of disturbance history and climate on carbon and water budgets in evergreen needleleaf forests. Agric. For. Meteorol. 113, 185–222.
Thornton, P.E., Running, S.W., 1999. An improved algorithm for estimating incident daily solar radiation from measurements of temperature, humidity, and precipitation. Agric. For. Meteorol. 93, 211–228.
Turner, B.L., Skole, D., Sanderson, S., Gunther, F., Louise, F., Leemans, R., 1995. Scope and Main Subjects of LUCC. Land-Use and Land-Cover Change Science/Research Plan. Stockholm and Geneva. International Geosphere-Biosphere Program and International Human Dimensions Programme (Rpt No. 7), 132 pp.
Urban, D., Keitt, T., 2001. Landscape connectivity: a graph-theoretic perspective. Ecology 82, 1205–1218.
Van Aardenne, J.A., Dentener, F.J., Olivier, J.G.J., Klein Goldewijk, C.G.M., Lelieveld, J., 2001. A 1×1 degree resolution dataset of historical anthropogenic trace gas emissions for the period 1890–1990. Global Biogeochem. Cycles 15, 909–928.
White, M.A., Thornton, P.E., Running, S.W., Nemani, R.R., 2000. Parameterization and sensitivity analysis of the BIOME-BGC terrestrial ecosystem model: net primary production controls. Earth Interact. 4, 1–85.
Whittaker, R.H., 1975. Communities and Ecosystems. Macmillan, New York, 385 pp.
Yadav, V., Malanson, G., 2008. Spatially explicit historical land use land cover and soil organic carbon transformations in Southern Illinois. Agric. Ecosyst. Environ. 123, 280–292.
Yadav, V., Del Grosso, S.J., Parton, W.J., Malanson, G.P., 2008. Adding ecosystem function to agent-based land use models. J. Land Use Sci. 3, 27–40.
Zhao, T., Brown, D.G., Bergen, K.M., 2007. Increasing gross primary production (GPP) in the urbanizing landscapes of Southeastern Michigan. Photogr. Eng. Remote Sens. 73, 1159–1167.